The Air-sea Carbon Dioxide Exchange over Tropical Pacific Ocean

1. Introduction

Large amounts of greenhouse gases (e.g., CO_2) have been released into the atmosphere since the industrial revolution. This emission is mainly the result of human activities, such as burning fossil fuels. The increased concentration of CO_2 in the atmosphere can cause serious consequences such as global warming. Both ocean and terrestrial ecosystems can absorb CO_2 from the atmosphere and are considered to moderate the process of global warming (Sabine et al., 2004; Doney et al., 2009, 2014; Le Quéré et al., 2009, 2010, 2016).

The tropical ocean can be considered a source of carbon dioxide (CO_2) in the atmosphere, and the mean emission is about 0.64 ± 0.22 Peta grams of carbon annually in the present decade (Ishii et al., 2014; Landschützer et al., 2014; Fay and Mckinley, 2013; Sarma et al., 2013; Schuster et al., 2013; Gruber et al., 2009; Feely et al., 2006). Among the tropical oceans, the Pacific Ocean plays an important role as a large sink for anthropogenic CO_2, which can partially mitigate the large-scale impact of humans emitting CO_2 into the atmosphere (Ishii et al., 2014). The Pacific Ocean also shows the spatial and temporal variability in the surface ocean pCO_2 (partial pressure of CO_2) and air-sea CO_2 fluxes on large-scale (Ishii et al., 2014; Messie and Chaves, 2013; Feely et al., 2002, 2006; Murtugudde et al., 1999). What's more, the El Niño-Southern Oscillation (ENSO) drives the major interannual variability in the tropical Pacific Ocean areas, which plays a dominant role in the interannual variability in global ocean CO_2 uptake (Ishii et al., 2014, Valsala et al., 2014).

However, quantifying the et air-sea CO_2 fluxes is still difficult due to the limited measurements in both space and time in many parts of the Ocean. What's more, the air-sea CO_2 fluxes can't be measured directly, which can involve lots of uncertainties in the derivation processes (Ishii et al., 2014). Comparing the observations with ocean models' simulation can improve the accuracy when assessing fluxes over large temporal and spatial scales. But the agreement among methods for estimating net air-sea CO_2 fluxes in the Pacific Ocean is relatively poor (McKinley et al., 2004; Peylin et al., 2005).

2. CO_2 fluxes estimation

2.1 Direct covariance flux method

The direct covariance measurement technique is the standard for the surface layer gas flux measurement. It is a direct calculation of the covariance of the gas concentration with vertical air velocity at the measurement height. Combined with the accurate estimation of the vertical velocity signal, the gas flux is calculated by correlating the actual vertical wind velocity with the atmospheric CO_2 concentration. Therefore, the accuracy of this flux depends on the sensitivity of the gas analyzer to high-frequency fluctuations. The rapid response measurements of CO_2 are used to estimate the CO_2 fluxes directly:

$$F_{CO_2} = \overline{w'c'} \text{ (McGillis et al., 2004),} \quad (1)$$

Where c' is the fluctuating atmospheric mixing ratio of CO_2 in dry air.

There are two main challenges when implementing the direct covariance flux method: (1) the presence of adequate fluctuation levels in w and c to calculate gas flux using currently available sensors, (2) the ability to remove the motion contamination and minimize the effect of flow distortion around an oceangoing vessel adequately. Momentum is very sensitive to momentum contamination as it requires correction for both vertical and horizontal velocities, unlike scalar flows including gas, which are affected primarily by vertical velocity uncertainties.

2.2 CO_2 flux profile method

The flux profile technique is based on the mean gradients of the atmospheric boundary layer, it offers several advantages for determining air-water fluxes. This method relies on measuring vertical gradients of CO_2 in the atmospheric surface layer. The flux profile method is related to the direct covariance flux by:

$$\overline{w'c'} = -K_c \frac{dc}{dz} \text{ (McGillis et al., 2004),} \quad (2)$$

Where K_c is the atmospheric diffusivity for CO_2, which can be defined as:

$$K_c = \frac{u_* \kappa z}{\emptyset_c(\xi)} \text{ (McGillis et al., 2004),} \quad (3)$$

Where $\emptyset_c$ is an empirically determined dimensionless gradient function for c, ξ is the stability parameter ($\xi = z/L$).

2.3 CO_2 bulk transfer method

The bulk transfer method provides an estimate for the fluxes between the ocean and the atmosphere. This method uses the mean, or bulk, change quantities and parameterized exchange rate. In the common bulk form, the CO_2 flux F_{CO_2} can be expressed as:

$$F_{CO_2} = k_{660} \Delta CO_{2aq} (Sc_{CO_2}/660)^{-n} \text{ (McGillis et al., 2004),} \quad (4)$$

Where k_{660} is the gas transfer velocity (Sc = 660), ΔCO_{2aq} is the difference of the concentration of aqueous dissolved CO_2 between the bulk seawater and the ocean surface, Sc_{co_2} is the CO_2 Schmidt number, and n is a hydrodynamic variable that is adjusted for flow condition.

3. Overview of air-sea CO_2 flux in the tropical Pacific

In the tropical Pacific, the physical and biogeochemical properties in the surface layer show a larger contrast between the domains of the western "warm pool" and the eastern "cold tongue" (Figs. 1 and 2).

The warm pool is characterized by high sea surface temperature (SST > 29.5 °C) and low sea surface salinities (SSS < 34.8), which is caused by the large solar heat influx and high annual precipitation. Due to the stratification, nitrate is depleted, and the concentration of dissolved inorganic carbon (DIC) is low (< 1950 μmol/kg at S = 35) in the surface layer. Besides, the net air-sea CO_2 fluxes over the "warm pool" are relatively small (< 1 mmol/m^{2}day) due to the near equilibration of surface water pCO_2 with the atmospheric CO_2, and the presence of low wind speeds.

The cold tongue is characterized by lower SST (22 °C < T < 29 °C) and higher SSS (> 35). In contrast, the eastern tropical Pacific cold tongue tends to be highly supersaturated with respect to atmospheric CO_2. This is caused by the wind-driven equatorial divergence and turbulent mixing that brings cooler, saline, nutrient- and CO_2-rich subsurface waters to the surface. The DIC concentration is higher (> 1980 µmol/kg at S = 35) than in the western Pacific warm pool (Figs. 1 and 2). During poleward and westward advection, most of the DIC in the upwelling is either removed by biological uptake or released into the atmosphere. However, due to the effect of simultaneous warming, CO_2 partial pressure in surface seawater (pCO_2sw) remains higher than in the atmosphere (pCO_2sw- pCO_2air > 90 µatm).

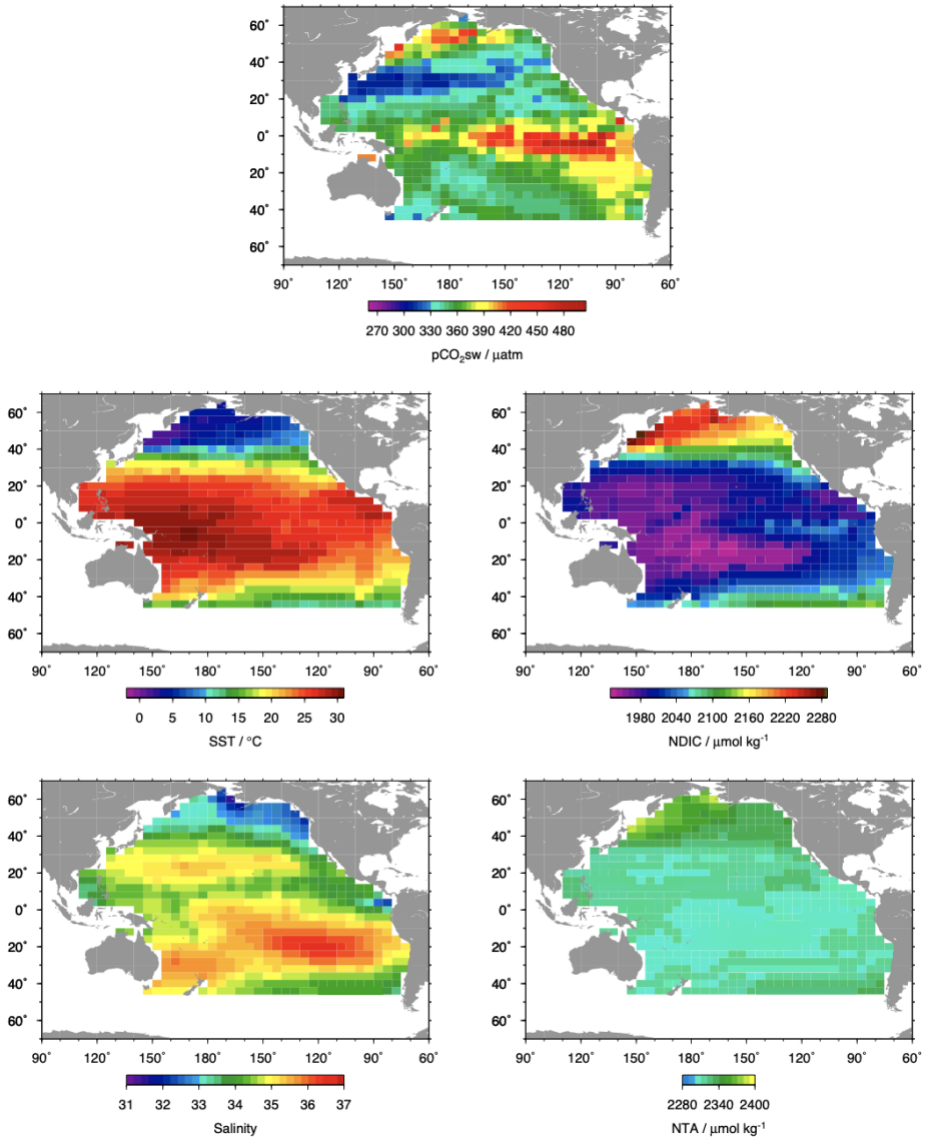

Fig. 1. Data-based climatology in February of pCO_2sw (top panel), temperature (middle left), salinity (bottom left) from LDEO V2009 (Takahashi et al., 2009), and salinity-normalized (S = 35) DIC (middle right) calculated with total alkalinity derived from Lee et al. (2006) (bottom right) (Ishii et al., 2014).

ENSO can drive the change in the distributions of DIC, SST, and salinity in both the surface water and wind field, During the cold events (La Niña), the "cold tongue" in the eastern tropic extends to the west. While during the warm events (El Niño), the "cold tongue" retreats to the east. ENSO can also cause large perturbations to pCO_2sw and significant temporal variations in the CO_2 outgassing from the tropical Pacific.

For the tropical Pacific, the large interannual variability is due to the global increasing trend of pCO_2sw in recent decades (Feely et al., 1999, 2006; Takahashi et al., 2003). The mean increase rate of pCO_2sw is consistent with the increase rate of atmospheric CO_2 (Takahashi et al., 2003; Feely et al., 2006; Ishii et al., 2009). But the decadal modulations reveal that the decadal variability of pCO_2sw possibly links with changes in the shallow meridional overturning circulation (McPhaden and Zhang, 2002, 2004).

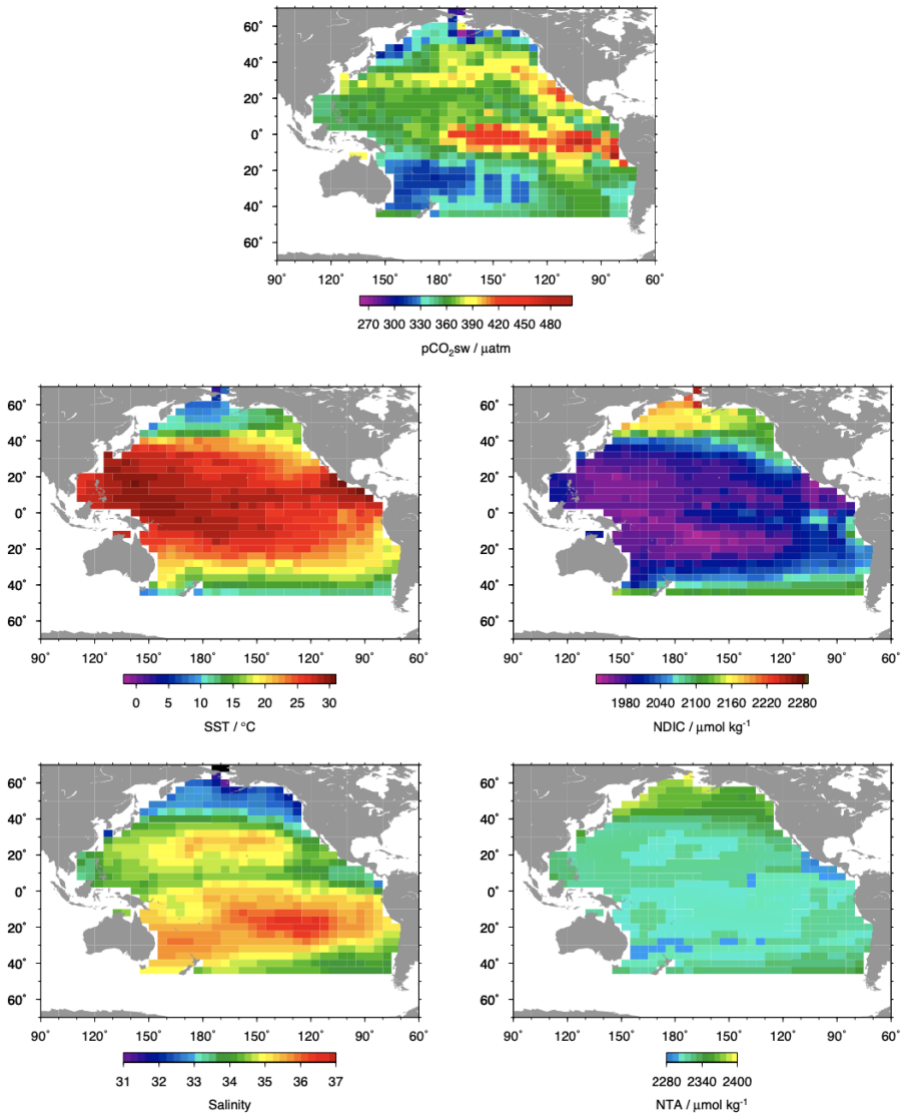

Fig. 2. Same as Fig. 1 but in August (Ishii et al., 2014).

4. Climate impacts

4.1 El Niño

The major interannual variability of CO_2 fluxes in the tropical Pacific is driven by ENSO. During the El Niño events, the tropical Pacific acts as a weak source of CO_2; during the La Niña events, the tropical Pacific acts as a strong source of CO_2 (Feely et al., 1999). The induced convergence caused by El Niño events can suppress the upwelling of CO_2-rich water and cause a reduction in the surface ocean carbon content in the central and eastern equatorial Pacific (Picaut et al., 1997). The DIC-depleted water can be advected from the western Pacific to the central and eastern Pacific, which can cause a reduction in oceanic pCO_2 (Cosca et al., 2003).

The Ocean Tracer Transport Model (OTTM; Valsala et al., 2008) is used as a physical model. The physical model calculates the evolution of passive tracers in the ocean by solving the advection-diffusion-source-sink equation on a spherical coordinate geometry. The necessary physical inputs for the model are temperature, salinity, ocean currents, surface heat, fresh water, and river fluxes. The offline data is taken from GFDL's coupled ocean-atmosphere reanalysis from 1961 to 2005 (ECDv3.1; Chang et al., 2013).

The model simulated annual mean pattern of CO_2 flux corresponds well with the Takahashi data over the period from 1990 to 2005 (Fig. 3). The CO_2 source over tropical Pacific is slightly over-estimated with the mean value of 0.89 ± 0.13 PgC/yr, which is nearly the double of the estimation from REgional Carbon Cycle Assessment and Processes (RECCAP), which value is 0.44 ± 0.14 PgC/yr (Ishii et al., 2014). But this mean value simulated by OTTM is close to other model estimates (e.g., McKinley et al., 2004).

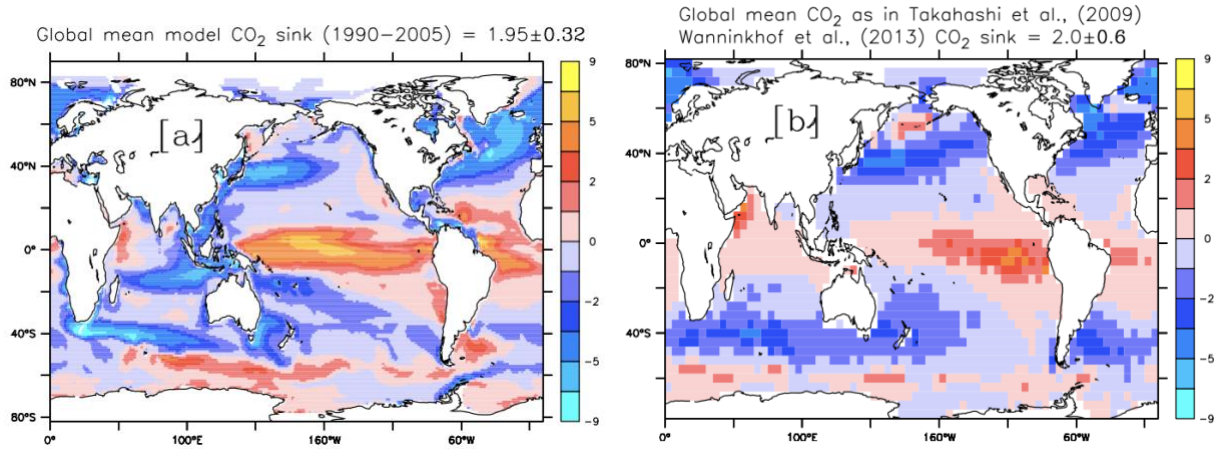

Fig. 3. (a) 1990-2005 average of global ocean surface sea-to-air CO_2 fluxes from the model. The global total sink during this period is 1.95 ± 0.32 PgC/yr. (b) Sea-to-air CO_2 fluxes from Takahashi et al., 2009 database. Units are in moles/m^2yr (Valsala, et al., 2014).

The EOFs method is used when resolving the seasonal evolution of SST during ENSO events in the equatorial Pacific. The results show that EOF-1 (calculated over 1961-2005) clearly captures the seasonal progression of SST anomalies during the ENSO event (Fig. 4). The SST anomalies

evolve from February-March of Year:0 and terminate in April of Year:+1, and begin to cool thereafter. The EOF of CO_2 flux anomalies (Fig. 4a) shows a peak between 160 °W and 120 °W from June of Year:0 to January of Year:+1. El Niño induces this type of change, as shown by the significant correlation between PC-1 (Fig. 4b) and the Niño 3.4 Index between these longitudes (Fig. 4c). Both the PC1-El Niño correlation and PC1-El Niño-Modoki correlation show significant correlations with the variation (Fig.4c). In Fig. 4b, positive values indicate a source and the multiplication of EOF-1 with PC-1 has the sigh of interannual variability. PC-1 is negative during 1982-1983 and 1997-1998, which suggests a negative CO_2 flux anomaly indicating a weaker CO_2 source or near-neutral condition extending almost from 150 °E to 90 °W. PC also shows a propagating nature from the central to the east Pacific (Fig. 4b).

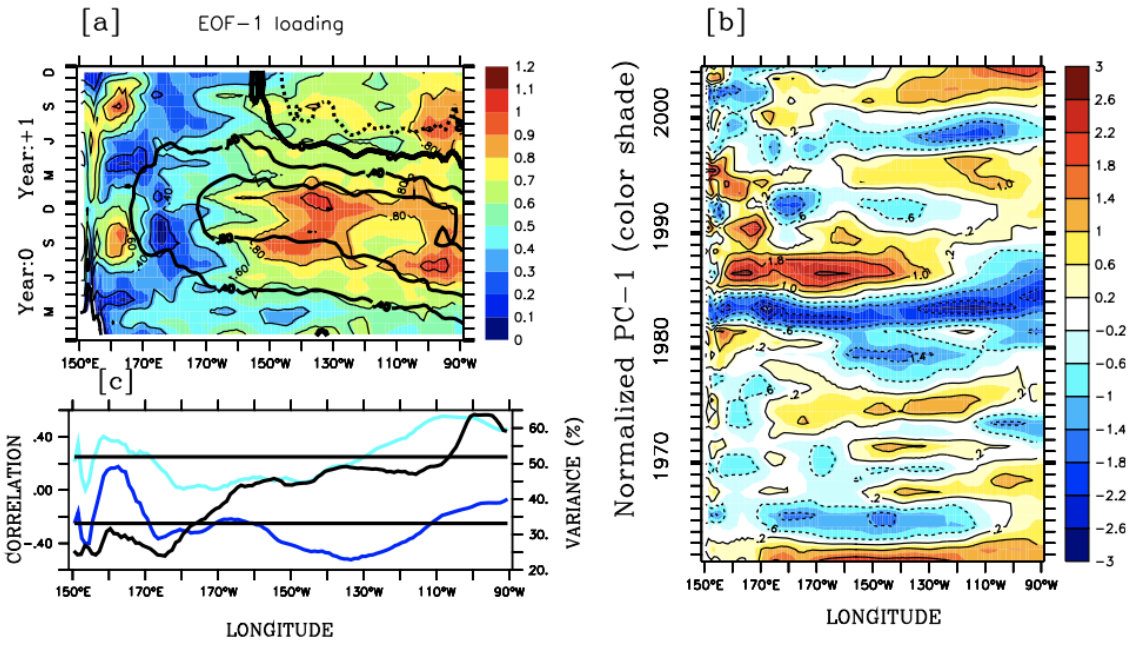

Fig. 4. (a) Seasonal evolutions of the dominant mode of interannual variability (shown over 2 years) of the equatorial Pacific CO_2 flux anomalies for each grid point from 160 °E to 90 °W (EOF-1). Color shade represents CO_2 flux (mol/m^{2}yr) and thick contour represents the corresponding EOF-1 of SST anomalies (°C). (b) the principle components (PC-1; normalized) for each grid point from 160 °E to 90 °W. (c) Time correlation between PC-1 and Niño 3.4 (blue) and El Niño-Modoki (cyan) from each grid point (left axis). The thick black line shows the variance explained by EOF-1 from each grid point (right axis) (Valsala et al., 2014).

The EOF-1 pattern in Fig. 4a is averaged over 150 °W to 110 °W in order to illustrate the detailed seasonal evolution of CO_2 flux anomalies (Fig. 5). In the tropical Pacific, the CO_2 flux anomalies co-evolve with SST anomalies during the El Niño events. The PC-1 needs to be multiplied with the EOF-1 in Fig. 5a in order to extract the nature of CO_2 evolution during any particular El Niño year.

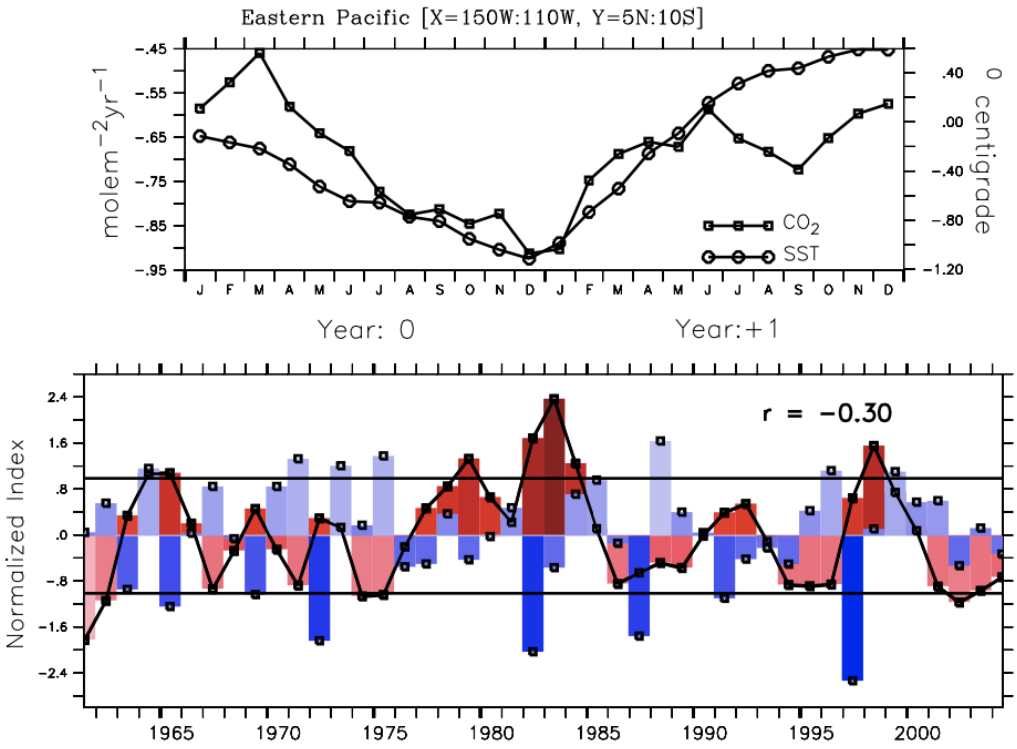

Fig. 5. (a) Seasonal evolutions of the dominant interannual sea-air CO_2 flux anomalies (left axis) and SST anomalies (right axis) from the central-to-east Pacific (spatially averaged between 150 °W and 110 °W) and shown for Year:0 and Year:+1. (b) The PC-1 of CO_2 flux anomalies (red bars and thick black line) and SST anomalies (blue bars). EOF-1 and PC-1 of SST have been reversed in the sign for easy comparison. The correlation coefficient between PC-1 of CO_2 flux and SST is shown (Valsala et al., 2014).

The corresponding EOFs of pCO_2 anomalies show a slightly different pattern of seasonal evolutions in the tropical Pacific (Fig. 6). The decoupling of pCO_2 and air-sea CO_2 flux variability can be caused by the wind-induced interannual variability in the CO_2 fluxes, which has the spatial and temporal dependencies. And this can induce a nonlinearity in the CO_2 flux-pCO_2 relationship. Besides, the SST and solubility could be other possible reasons for inducing the nonlinearity in the pCO_2-CO_2 flux relations. EOF-1 shows generally a single sign of anomalies of pCO_2 over the entire equatorial Pacific during El Niño years (Fig. 6a). The largest pCO_2 anomaly does not show any significant east-to-east proportion in PC-1 which differs from the CO_2 fluxes (Fig. 6b).

The pCO_2 shows a distinct response to El Niño-Modoki, especially in the western Pacific (to the west of 150 °W). The correlation between PC-1 and El Niño is weaker between 150 °E and 150 °W, while the correlation between PC-1 and El Niño-Modoki is higher (Fig. 6c). It is not surprising that pCO_2 shows strong variability in response to El Niño events and their different types, whereas CO_2 flux is comminated by typical El Niño alone. This suggests a non-linear role for wind inducing the CO_2 flux-pCO_2 relationship.

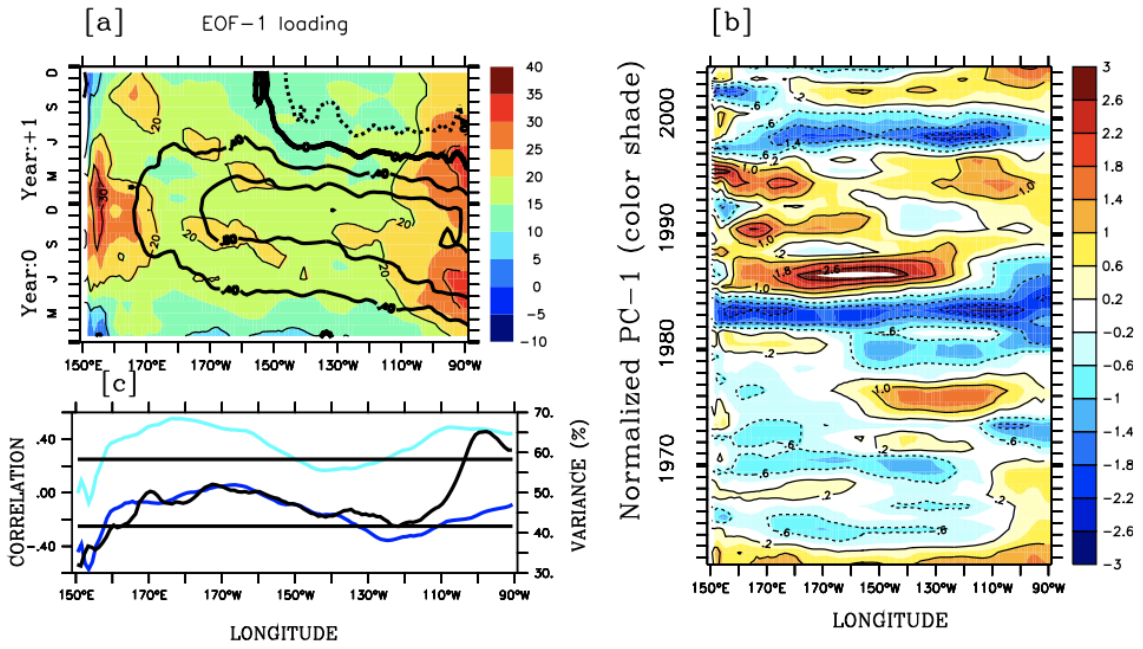

Fig. 6. Same as Fig. 4, but for pCO_2 anomalies (units: µatm) (Valsala et al., 2014).

4.2 Precipitation

On the short time scales, the flux of CO_2 between the atmosphere and the ocean (F_{CO_2}) is controlled by the gas transfer velocity (Kco_2), and the difference in the pCO_2 in the water and the atmosphere (Δp_{CO_2}) can be expressed by:

$$F_{CO_2} = k_{CO_2} K_0 \Delta p_{CO_2} \text{ (Ho \& Schanze, 2020),} \quad (5)$$

Where K_0 is the solubility coefficient for CO_2, which varies as a function of water temperature and salinity (Weiss, 1974).

Rain has been proven to increase k_{CO_2} in both fresh and salt water (Ho et al., 2004; Takagaki & Komori, 2007; Zappa et al., 2009), and it could also result in the increase of F_{CO_2}. Other processes such as the cool skin effects, microlayer salinity anomaly, and diurnal warming and warming layer effect can also affect the F_{CO_2}. What's more, rain can dilute DIC and total alkalinity (TAlk) of the surface ocean as it contains negligible TAlk and a small amount of DIC compared to the surface ocean. This process can result in the lowering of pCO_2 in the surface water (Turk et al., 2010). This effect can increase the ocean uptake of atmospheric CO_2 as it would make Δp_{CO_2} (e.g., surface ocean pCO_2 minus atmospheric pCO_2) more negative in sink regions (e.g., surface ocean pCO_2 is lower than the atmosphere) and make Δp_{CO_2} less positive in source regions (e.g., surface ocean pCO_2 is higher than the atmosphere). However, the rain-lowering surface ocean pCO_2 through dilution has not been fully studied until now. It is mainly because the air intakes of ships where pCO_2 measurements are being taken are usually located far below the water surface (at a depth of 5-m or more).

The measurements were taken aboard the Research Vessel Roger Revelle (R/V Roger Revelle) as a part of the Salinity Processes in the Upper Ocean Regional Study 2 (SPURS-2) (Lindstrom et al., 2019) from 16 October to 17 November 2017 (including transit to the study site). And the goal of SPURS-2 was to understand the physical processes controlling the sinks and sources of freshwater in the ocean.

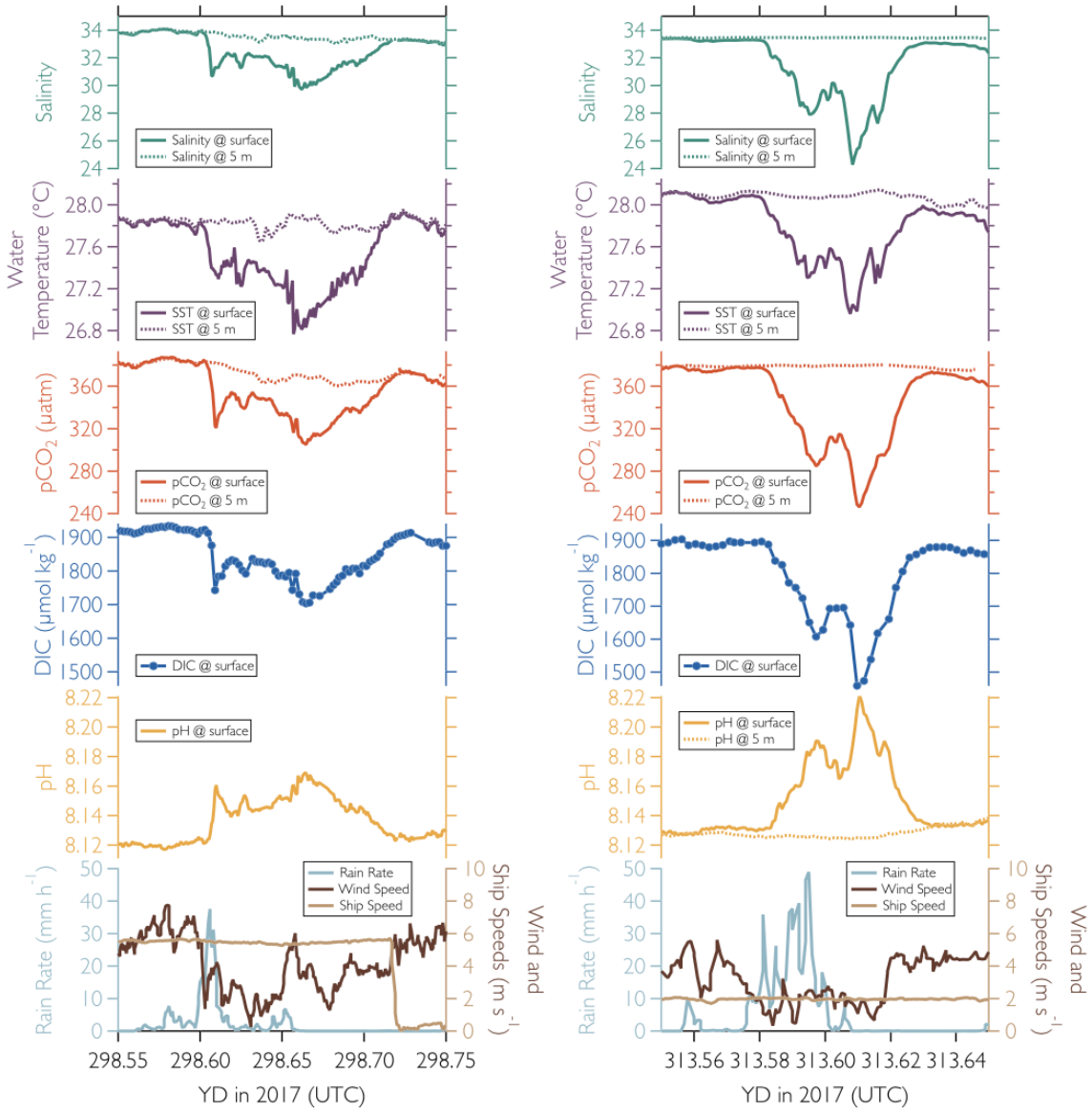

Fig. 7. Time series of salinity, water temperature, pCO_2, DIC, pH, rain rate, wind speed, and ship speed for two of the puddles encountered during SPURS-2. Waterside parameters from the Salinity Snake and from the 5-m intake of the ship are shown where available. All parameters were measured, except pCO_2 from the Salinity Snake, which was calculated from measured DIC and pH. No pH measurements were available from the 5-m water intake on YD 298 (Ho & Schanze, 2020).

During SPURS-2, 8 large freshwater pools ("puddles") are defined when the difference of the measured salinity between the Salinity Snake (a specially designed system) and the 5-m intake of the ship is more than 0.5 over a few km. Since the starting DIC and TAlk were similar for all puddles, the resulting changes in pCO_2 due to rain were also similar. Here, two larger puddles are studied, one from YD 298 (October 25, 2017) and another from YD 313 (November 9, 2017). Both of these two puddles are characterized by a decrease in SSS of up to 4.4, a decrease in SST of 1.3 °C, and a decrease in pCO_2 of 84 μatm (Fig. 7).

Comparing the measurements of the surface and 5-m instruments, it is clear that rain can dilute the SSS significantly. This dilution can affect the carbonate system parameters as well. During both YD 298 and YD 313, the surface salinity dropped rapidly when the ship encountered these two puddles (Fig. 7). This drop was accompanied by rapid change of surface pCO_2, DIC, and PH, compared with the 5-m depth measurements.

Also, the rain rate has shown that the rain had largely stopped during the YD 298 puddle transect, while there was still raining pretty heavily during the early part of the YD 313 puddle (Fig. 7). This difference in the rain conditions indicates how long the surface anomalies must mix to drop down to 5 m. On YD 298, salinity and pCO_2 (and other parameters) changes were shown even from the instrument at 5 m, although not as much.

Besides the effect of adding freshwater to the sea surface that lowers the salinity, rain is often cooler than seawater, which can cause a decrease in SST. Both can change the sea surface pCO_2. For example, the maximum salinity changes of the puddles YD 298 and 313 were 4.4 and 9.3 respectively, while the SST change was 1.3 °C for both puddles. For the puddles YD 298 and 313, the observed decreases in pCO_2 were 84 and 135 μatm respectively. There is a nearly 88% decrease for YD 298 and a 93% decrease for YD 313, which were caused by both the salinity dilution and temperature changes.

5. Summary

The air-sea CO_2 fluxes over the Pacific Ocean are characterized by large-scale structures that relate to various factors such as ocean subduction, upwelling patterns, combined effects of wind-driven gas exchange, and biology. The tropical Pacific is considered a large sink of anthropogenic CO_2 in the atmosphere. From the large-scale, the Pacific Ocean also shows spatial and temporal variability in the air-sea CO_2 fluxes. The cold and warm events of ENSO can result in positive and negative anomalies of the air-sea CO_2 fluxes Regarding the interannual variability.

The major interannual variability of CO_2 fluxes in the tropical Pacific is driven by ENSO. The tropical Pacific acts as a weak source of CO_2 during the El Niño events, while during the La Niña events, the tropical Pacific acts as a strong source of CO_2. The El Niño events can induce convergence, which can suppress the upwelling of CO_2-rich water and cause the reduction in the surface ocean carbon content in the central and eastern tropical Pacific. The fact that pCO_2 shows strong variability in response to El Niño events and their different types is not surprising. However, unlike the pCO2, the CO2 flux is influenced only by the typical El Niño along, suggesting a non-linear role for wind inducing the CO_2 flux-pCO_2 relationship.

Despite El Niño, precipitation is another factor that influences the air-sea CO_2 fluxes. Previous studies have proven that rain can increase CO_2 transfer velocity in both fresh and salt water, which can also increase the flux of CO_2 between the atmosphere and the ocean. Also, rain can dilute the DIC and TAlk of the surface ocean, which can increase the ocean uptake of atmospheric CO_2. Except for the effect of adding freshwater to the sea surface which can lower the salinity, rain can cause a decrease in SST as it is often cooler than seawater. And both these two effects can change the sea surface pCO_2.

Reference

Chang, Y.-S., Zhang, S., Rosati, A., Delworth, T. L., & Stern, W. F. (2013). An assessment of oceanic variability for 1960–2010 from the GFDL ensemble coupled data assimilation. Climate Dynamics, 40(3-4), 775–803. https://doi.org/10.1007/s00382-012-1412-2

Cosca, C. E., Feely, R. A., Boutin, J., Etcheto, J., McPhaden, M. J., Chavez, F. P., & Strutton, P. G. (2003). Seasonal and interannual CO2 fluxes for the central and eastern equatorial Pacific Ocean as determined from fCO2-SST relationships. Journal of Geophysical Research - Oceans, 108(C8), 3278–n/a. https://doi.org/10.1029/2000JC000677

Doney, S., Balch, W., Fabry, V., & Feely, R. (2009). OCEAN ACIDIFICATION: A CRITICAL EMERGING PROBLEM FOR THE OCEAN SCIENCES. Oceanography (Washington, D.C.), 22(4), 16–25. https://doi.org/10.5670/oceanog.2009.93

Doney, S., Bopp, L., & Long, M. (2014). Historical and Future Trends in Ocean Climate and Biogeochemistry. Oceanography (Washington, D.C.), 27(1), 108–119. https://doi.org/10.5670/oceanog.2014.14

Fay, A. R., & McKinley, G. A. (2013). Global trends in surface ocean pCO2 from in situ data. Global Biogeochemical Cycles, 27(2), 541–557. https://doi.org/10.1002/gbc.20051

Feely, R. A., Boutin, J., Cosca, C. E., Dandonneau, Y., Etcheto, J., Inoue, H. Y., Ishii, M., Quéré, C. L., Mackey, D. J., McPhaden, M., Metzl, N., Poisson, A., & Wanninkhof, R. (2002). Seasonal and interannual variability of CO2 in the equatorial Pacific. Deep-Sea Research. Part II, Topical Studies in Oceanography, 49(13-14), 2443–2469. https://doi.org/10.1016/S0967-0645(02)00044-9

Feely, R. A., Takahashi, T., Wanninkhof, R., McPhaden, M. J., Cosca, C. E., Sutherland, S. C., & Carr, M.-E. (2006). Decadal variability of the air-sea CO2 fluxes in the equatorial Pacific Ocean. Journal of Geophysical Research - Oceans, 111(C8), C08S90–n/a. https://doi.org/10.1029/2005JC003129

Feely, R. A., Wanninkhof, R., Takahashi, T., & Tans, P. (1999). Influence of El Niño on the equatorial Pacific contribution to atmospheric CO2 accumulation. Nature (London), 398(6728), 597–601. https://doi.org/10.1038/19273

Gruber, N., Gloor, M., Mikaloff Fletcher, S. E., Doney, S. C., Dutkiewicz, S., Follows, M. J., Gerber, M., Jacobson, A. R., Joos, F., Lindsay, K., Menemenlis, D., Mouchet, A., Müller, S. A., Sarmiento, J. L., & Takahashi, T. (2009). Oceanic sources, sinks, and transport of atmospheric CO2. Global Biogeochemical Cycles, 23(1), GB1005–n/a. https://doi.org/10.1029/2008GB003349

Ho, D. T., & Schanze, J. J. (2020). Precipitation-Induced Reduction in Surface Ocean pCO2: Observations From the Eastern Tropical Pacific Ocean. Geophysical Research Letters, 47(15). https://doi.org/10.1029/2020GL088252

Ho, D. T., Zappa, C. J., McGillis, W. R., Bliven, L. F., Ward, B., Dacey, J. W. H., Schlosser, P., & Hendricks, M. B. (2004). Influence of rain on air-sea gas exchange: Lessons from a model ocean. Journal of Geophysical Research - Oceans, 109(C8), C08S18–n/a. https://doi.org/10.1029/2003JC001806

Ishii, M., Feely, R. A., Rodgers, K. B., Park, G.-H., Wanninkhof, R., Sasano, D., Sugimoto, H., Cosca, C. E., Nakaoka, S., Telszewski, M., Nojiri, Y., Fletcher, S. E. M., Niwa, Y., Patra, P. K., Valsala, V., Nakano, H., Lima, I., Doney, S. C., Buitenhuis, E. T., … Takahashi, T. (2014). Air-sea CO2 flux in the Pacific Ocean for the period 1990-2009. Biogeosciences, 11(3), 709–734. https://doi.org/10.5194/bg-11-709-2014

Ishii, M., Inoue, H. Y., Midorikawa, T., Saito, S., Tokieda, T., Sasano, D., Nakadate, A., Nemoto, K., Metzl, N., Wong, C. S., & Feely, R. A. (2009). Spatial variability and decadal trend of the oceanic CO2 in the western equatorial Pacific warm/fresh water. Deep-Sea Research. Part II, Topical Studies in Oceanography, 56(8-10), 591–606. https://doi.org/10.1016/j.dsr2.2009.01.002

Landschützer, P., Gruber, N., Bakker, D. C. E., & Schuster, U. (2014). Recent variability of the global ocean carbon sink. Global Biogeochemical Cycles, 28(9), 927–949. https://doi.org/10.1002/2014GB004853

Le Quéré, C., Anew, R. M., Canadell, J. G., Sitch, S., Korsbakken, J. I., Peters, G. P., Manning, A. C., Boden, T. A., Tans, P. P., Houghton, R. A., Keeling, R. F., Alin, S., Anews, O. D., Anthoni, P., Barbero, L., Bopp, L., Chevallier, F., Chini, L. P., Ciais, P., … Friedlingstein, P. (2016). Global Carbon Budget 2016. Earth System Science Data, 8(2), 605–649. https://doi.org/10.5194/essd-8-605-2016

Le Quéré, C., Canadell, J. G., Marland, G., & Raupach, M. R. (2009). Trends in the sources and sinks of carbon dioxide. Nature Geoscience, 2(12), 831–836. https://doi.org/10.1038/ngeo689

Le Quéré, C., Takahashi, T., Buitenhuis, E. T., Rödenbeck, C., & Sutherland, S. C. (2010). Impact of climate change and variability on the global oceanic sink of CO2. Global Biogeochemical Cycles, 24(4). https://doi.org/10.1029/2009GB003599

Lee, K., Tong, L. T., Millero, F. J., Sabine, C. L., Dickson, A. G., Goyet, C., Park, G.-H., Wanninkhof, R., Feely, R. A., & Key, R. M. (2006). Global relationships of total alkalinity with salinity and temperature in surface waters of the world's oceans. Geophysical Research Letters, 33(19), L19605–n/a. https://doi.org/10.1029/2006GL027207

Lindstrom, E., Bryan, F., & Schmitt, R. (2015). SPURS: Salinity Processes in the Upper-ocean Regional Study: THE NORTH ATLANTIC EXPERIMENT. Oceanography (Washington, D.C.), 28(1), 14–19. https://doi.org/10.5670/oceanog.2015.01

McGillis, W. R., Edson, J. B., Hare, J. E., & Fairall, C. W. (2001). Direct covariance air-sea CO2 fluxes. Journal of Geophysical Research: Oceans, 106(C8), 16729–16745. https://doi.org/10.1029/2000JC000506

McGillis, W. R., Edson, J. B., Zappa, C. J., Ware, J. D., McKenna, S. P., Terray, E. A., Hare, J. E., Fairall, C. W., Drennan, W., Donelan, M., DeGrandpre, M. D., Wanninkhof, R., & Feely, R. A. (2004). Air-sea CO2 exchange in the equatorial Pacific. Journal of Geophysical Research - Oceans, 109(C8), C08S02–n/a. https://doi.org/10.1029/2003JC002256

McKinley, G. A., Follows, M. J., & Marshall, J. (2004). Mechanisms of air-sea CO2 flux variability in the equatorial Pacific and the North Atlantic. Global Biogeochemical Cycles, 18(2), GB2011–n/a. https://doi.org/10.1029/2003GB002179

McPhaden, M. J., & Zhang, D. (2002). Slowdown of the meridional overturning circulation in the upper Pacific Ocean. Nature (London), 415(6872), 603–608. https://doi.org/10.1038/415603a

McPhaden, M. J., & Zhang, D. (2004). Pacific Ocean circulation rebounds. Geophysical Research Letters, 31(18), L18301–n/a. https://doi.org/10.1029/2004GL020727

Messié, M., & Chavez, F. P. (2013). Physical-biological synchrony in the global ocean associated with recent variability in the central and western equatorial Pacific. Journal of Geophysical Research. Oceans, 118(8), 3782–3794. https://doi.org/10.1002/jgrc.2027

Murtugudde, R. G., Signorini, S. R., Christian, J. R., Busalacchi, A. J., McClain, C. R., & Picaut, J. (1999). Ocean color variability of the tropical Indo-Pacific basin observed by SeaWiFS during 1997-1998. Journal of Geophysical Research, Washington, DC, 104(C8), 18351–18366. https://doi.org/10.1029/1999JC900135

Peylin, P., Bousquet, P., Le Quéré, C., Sitch, S., Friedlingstein, P., McKinley, G., Gruber, N., Rayner, P., & Ciais, P. (2005). Multiple constraints on regional CO2 flux variations over land and oceans. Global Biogeochemical Cycles, 19(1), GB1011–n/a. https://doi.org/10.1029/2003GB002214

Picaut, J., Masia, F., & Di Penhoat, Y. (1997). An Advective-Reflective Conceptual Model for the Oscillatory Nature of the ENSO. Science, 277(5326), 663–666. https://doi.org/10.1126/science.277.5326.663

Sabine, C. L., Feely, R. A., Millero, F. J., Peng, T.-H., Kozyr, A., Ono, T., Rios, A. F., Gruber, N., Key, R. M., Lee, K., Bullister, J. L., Wanninkhof, R., Wong, C. S., Wallace, D. W. R., & Tilbrook, B. (2004). The Oceanic Sink for Anthropogenic CO2. Science (American Association for the Advancement of Science), 305(5682), 367–371. https://doi.org/10.1126/science.1097403

Sarma, V. V. S. S., Lenton, A., Law, R. M., Metzl, N., Patra, P. K., Doney, S., Lima, I. D., Dlugokencky, E., Ramonet, M., & Valsala, V. (2013). Sea-air CO2 fluxes in the Indian Ocean between 1990 and 2009. Biogeosciences, 10(11), 7035–7052. https://doi.org/10.5194/bg-10-7035-2013

Schuster, U., McKinley, G. A., Bates, N., Chevallier, F., Doney, S. C., Fay, A. R., González-Dávila, M., Gruber, N., Jones, S., Krijnen, J., Landschützer, P., Lefèvre, N., Manizza, M., Mathis, J., Metzl, N., Olsen, A., Rios, A. F., Rödenbeck, C., Santana-Casiano, J. M., … Watson, A. J. (2013). An assessment of the Atlantic and Arctic sea-air CO2 fluxes, 1990-2009. Biogeosciences, 10(1), 607–627. https://doi.org/10.5194/bg-10-607-2013

Takagaki, N., & Komori, S. (2007). Effects of rainfall on mass transfer across the air-water interface. Journal of Geophysical Research, 112(C6), C06006–n/a. https://doi.org/10.1029/2006JC003752

Takahashi, T., Sutherland, S. C., Feely, R. A., & Cosca, C. E. (2003). Decadal variation of the surface water PC[O.sub.2] in the western and central equatorial Pacific. Science (American Association for the Advancement of Science), 302(5646), 852–.

Takahashi, T., Sutherland, S. C., Wanninkhof, R., Sweeney, C., Feely, R. A., Chipman, D. W., Hales, B., Friederich, G., Chavez, F., Sabine, C., Watson, A., Bakker, D. C. ., Schuster, U., Metzl, N., Yoshikawa-Inoue, H., Ishii, M., Midorikawa, T., Nojiri, Y., Körtzinger, A., … Baar, H. J. W. de. (2009). Climatological mean and decadal change in surface ocean pCO2, and net sea–air CO2 flux over the global oceans. Deep-Sea Research. Part II, Topical Studies in Oceanography, 56(8), 554–577. https://doi.org/10.1016/j.dsr2.2008.12.009

Turk, D., Zappa, C. J., Meinen, C. S., Christian, J. R., Ho, D. T., Dickson, A. G., & McGillis, W. R. (2010). Rain impacts on CO2 exchange in the western equatorial Pacific Ocean. Geophysical Research Letters, 37(23). https://doi.org/10.1029/2010GL045520

Valsala, V. K., Roxy, M. K., Ashok, K., & Murtugudde, R. (2014). Spatiotemporal characteristics of seasonal to multidecadal variability of pCO2 and air-sea CO2 fluxes in the equatorial Pacific Ocean. Journal of Geophysical Research. Oceans, 119(12), 8987–9012. https://doi.org/10.1002/2014JC010212

Vinu Valsala, V., Maksyutov, S., & Ikeda, M. (2008). DESIGN AND VALIDATION OF AN OFFLINE OCEANIC TRACER TRANSPORT MODEL FOR CARBON CYCLE STUDY. In [np]. 2-7 Mar 2008.

Weiss, R. F. (1974). Carbon dioxide in water and seawater: the solubility of a non-ideal gas. Marine Chemistry, 2(3), 203–215. https://doi.org/10.1016/0304-4203(74)90015-2

Zappa, C. J., Ho, D. T., McGillis, W. R., Banner, M. L., Dacey, J. W. H., Bliven, L. F., Ma, B., & Nystuen, J. (2009). Rain-induced turbulence and air-sea gas transfer. Journal of Geophysical Research, 114(C7), C07009–n/a. https://doi.org/10.1029/2008JC005008